Eur. Phys. J. B **59**, 435–445 (2007)
DOI: 10.1140/epjb/e2007-00051-5

THE EUROPEAN PHYSICAL JOURNAL B

Analytical study of magnetization dynamics driven by spin-polarized currents

R. Bonin[1,a], C. Serpico[2], G. Bertotti[1], I.D. Mayergoyz[3], and M. d'Aquino[4]

[1] Istituto Nazionale di Ricerca Metrologica, Strada delle Cacce 91, 10135 Torino, Italy
[2] Dipartimento di Ingegneria Elettrica, Università di Napoli "Federico II", via Claudio 21, 80125 Napoli, Italy
[3] Department of Electrical and Computer Engineering, University of Maryland, College Park MD 20742, USA
[4] Dipartimento per le Tecnologie, Università di Napoli "Parthenope", via Medina 40, 80133 Napoli, Italy

Received 29 September 2006 / Received in final form 25 Junuary 2007
Published online 16 February 2007 –

Abstract. An analytical approach is presented for the study of magnetization dynamics driven by spin-polarized currents. Two cases are considered: (i) magnetic layers with in-plane uniaxial anisotropy; (ii) magnetic layers with uniaxial anisotropy and applied field perpendicular to the layer plane. Theoretical predictions are obtained for the existence of stationary modes and self-oscillations of magnetization by solving the deterministic Landau-Lifshitz-Gilbert equation with Slonczewski spin-torque term. Thermal fluctuations are studied by deriving the corresponding Fokker-Planck equation for the magnetization probability distribution. Analytical procedures to estimate the effective potential barrier separating self-oscillatory regimes and/or stationary modes are proposed.

PACS. 75.60.Jk Magnetization reversal mechanisms – 85.70.Kh Magnetic thin film devices: magnetic heads

1 Introduction

As theoretically shown by Berger [1] and Slonczewski [2], the torque exerted by spin-polarized electrons can substantially influence the magnetization dynamics in a ferromagnetic nanoelement. This interaction, known as spin transfer arises when the linear dimensions of the ferromagnetic element are of the order of tens of nanometers and the current density is of the order of $\sim 10^7 \div 10^8$ A cm^{-2}.

After these theoretical predictions, several experiments were performed to investigate the magnetization dynamics in nanomagnets driven by the joint presence of spin-polarized currents and external magnetic fields [3–7]. In these experiments, carried out for both nanopillar structures and point-contact geometries, a rich variety of dynamical regimes were observed, namely, switching and self-oscillations of the magnetization with, in some cases, hysteretic transitions between stationary states and steady-state auto-oscillations. In parallel with these experimental investigations, a great deal of theoretical work has been developed to study phenomena directly related to spin-transfer [8–13].

Despite its quantum origin, the spin-transfer torque can be classically modeled by adding an appropriate term to the Landau-Lifshitz-Gilbert (LLG) equation [2] for the ferromagnetic element subject to the spin-polarized current. Solutions of this modified LLG equation can be obtained through numerical integration [14–16]. However, it has been shown that under the condition of spatially uniform magnetization, the modified LLG equation can be analytically solved [17–19]. Although they represent a particular case, spatially uniform solutions can be a good approximation to the magnetization dynamics in nanopillar devices, where the small spatial dimensions involved strongly penalize magnetization nonuniformities.

For the small volumes involved in spin-transfer devices, thermal fluctuations may induce transitions between different dynamical regimes, as shown by experimental observations [20–22]. To take into account the effect of temperature on the magnetization dynamics, a random torque term can be added to the modified LLG equation, in analogy to what was proposed by Brown [23] for the study of thermal fluctuations in fine particles. In these systems, when no spin-polarized current is injected, magnetization dynamics admit the coexistence of a certain number of stationary equilibrium states, and the effect of thermal fluctuations can be estimated by comparing the energy barrier separating these equilibria with k_BT (k_B is the Boltzmann constant and T the absolute temperature). In particular, in the limit of large energy barriers, the time scale of the thermal relaxation is given by the Arrhenius formula $\tau = \tau_0 \exp(\Delta E/k_BT)$, which expresses the relaxation time τ in terms of the height ΔE of the energy barrier and a characteristic time constant τ_0 (typically $\tau_0 \sim 10^{-10} \div 10^{-11}$s) [24,25]. The situation is drastically modified when the spin-polarized current is injected. In this case, self-oscillatory regimes may appear in addition

[a] e-mail: bonin@inrim.it

to stationary equilibria and thermal fluctuations can induce switching between these steady states of different nature. The main problem is to define the concept of effective potential barrier between a self-oscillatory regime and a stationary equilibrium, or between two oscillatory regimes.

An analytical approach to the study of thermal fluctuations in spin-torque devices was proposed by Li and Zhang [26]. Starting from a stochastic LLG equation with the spin-torque term, they derived the corresponding Fokker-Planck equation for the magnetization probability distribution [26]. They obtained that the stationary probability density corresponds to the Boltzmann distribution with an effective temperature which depends on the injected current. Finally they calculated the transition rates between two stationary equilibria. Apalkov and Visscher [27,28] proposed an approach based on a Fokker-Planck equation in energy [29]. By assuming that the magnetization probability density depends only on energy, they calculated the expression for the effective temperature which appears in the Boltzmann distribution for the stationary probability density. On the other hand, Krivorotov et al. [22] obtained experimental results which can be reasonably explained by assuming that thermal switching is activated and governed by the sample temperature and a current-dependent activation barrier rather than an effective temperature which depends on the current.

In this article, we describe a mathematical approach to study spin-torque-driven magnetization dynamics. In particular, we discuss an analytical treatment to describe magnetization dynamics in the deterministic case. In spite of the nontrivial mathematical structure of the deterministic LLG equation with the spin-torque term, this problem was solved by taking advantage of Poincaré-Melnikov theory for slightly dissipative nonlinear systems [18]. On this mathematical basis, it becomes possible to study analytically the occupation probability for stationary equilibria as well as self-oscillatory regimes [30,31]. In this two works it was proved that the stationary probability density is formally coincident with the Boltzmann distribution, but involves an effective potential which contains a non-equilibrium current-dependent part. Knowledge of this effective potential permits one to quantify the probability of occupation of each stationary state and the probability of transition between different states.

In Section 2, we describe the methods used for the analysis of spin-torque-driven magnetization dynamics in absence of fluctuations, to determine magnetization steady states, that is, stationary states and self-oscillations. In Section 3, by using the stochastic LLG equation, we investigate the occurrence of thermally induced magnetization switching between these different steady states. In particular, we obtain the expression for the effective potential which governs the stochastic process and for the transition rates from one steady state to another one. The approach discussed in these two Sections is applied to the case in which the ferromagnetic element is a thin film which presents in-plane anisotropy. Finally, in Section 4 we describe deterministic and stochastic dynamics in thin films with perpendicular anisotropy and uniaxial symmetry.

2 Deterministic dynamics

We consider, as in reference [2], a three-layer structure composed by two ferromagnetic layers separated by a non-magnetic spacer. The current passes through the layers in the direction perpendicular to the layers plane and it acquires a certain degree of spin polarization by interacting with the magnetization of the so-called "fixed-layer". This magnetization is assumed to be fixed along a given direction. Conversely, the magnetization of the "free-layer" exhibits various dynamical regimes induced by the spin-transfer torque. By following the approach developed by Slonczewski [2], the magnetization dynamics in the free-layer, whose magnetization is assumed to be spatially uniform, is described by the LLG equation with the addition of the spin-transfer torque. In dimensionless form, this equation is expressed as:

$$\frac{d\mathbf{m}}{dt} - \alpha\,\mathbf{m}\times\frac{d\mathbf{m}}{dt} = -\mathbf{m}\times\left(\mathbf{h}_{\text{eff}} - \beta\frac{\mathbf{m}\times\mathbf{e}_p}{1+c_p\mathbf{m}\cdot\mathbf{e}_p}\right), \quad (1)$$

where the free-layer magnetization $\mathbf{m}$ and the effective field $\mathbf{h}_{\text{eff}}$ are normalized by the saturation magnetization M_s, time is measured in units of $(\gamma M_s)^{-1}$ (γ is the absolute value of the gyromagnetic ratio), α is Gilbert damping constant (generally $\alpha \ll 1$), and the unit vector $\mathbf{e}_p$ gives the direction of the spin polarization. In the purely ballistic model originally proposed by Slonczewski [2], $c_p = (1+P)^3/[3(1+P)^3 - 16P^{3/2}]$ and $\beta = 4(J_e/J_p)P^{3/2}/[3(1+P)^3 - 16P^{3/2}]$, where P ($0 < P < 1$) is the degree of spin polarization in the ferromagnet, J_e is the electric current density, taken as positive when the electrons flow from the free into the fixed layer, and $J_p = \mu_0 M_s^2 |e| d/\hbar$ (μ_0 is the vacuum permeability, e is the electron charge, d is the thickness of the free layer, and $\hbar$ is reduced Planck constant). Typically, $J_p \simeq 10^9 \text{A cm}^{-2}$, which means that $\beta \ll 1$ for the typical current densities, $J_e \lesssim 10^8 \text{A cm}^{-2}$, employed in experiments. The effective field is given by $\mathbf{h}_{\text{eff}} = -\partial g_L/\partial\mathbf{m}$, where:

$$g_L(\mathbf{m};\mathbf{h}_a) = (D_x m_x^2 + D_y m_y^2 + D_z m_z^2)/2 - \mathbf{h}_a\cdot\mathbf{m} \quad (2)$$

is the free-layer energy density normalized by $\mu_0 M_s^2$. By assuming that both shape and crystal anisotropy have the same ellipsoid-like symmetry, we can describe their joint effect through the quadratic term in equation (2), whereas the linear term gives the interaction with the external field $\mathbf{h}_a$. It is useful for the following discussion to introduce the function:

$$\Phi_{ST}(\mathbf{m}) = \ln(1 + c_p\mathbf{m}\cdot\mathbf{e}_p)/c_p. \quad (3)$$

In terms of Φ_{ST}, equation (1) becomes:

$$\frac{d\mathbf{m}}{dt} - \alpha\mathbf{m}\times\frac{d\mathbf{m}}{dt} = \mathbf{m}\times\left(\frac{\partial g_L}{\partial\mathbf{m}} + \beta\,\mathbf{m}\times\frac{\partial\Phi_{ST}}{\partial\mathbf{m}}\right). \quad (4)$$

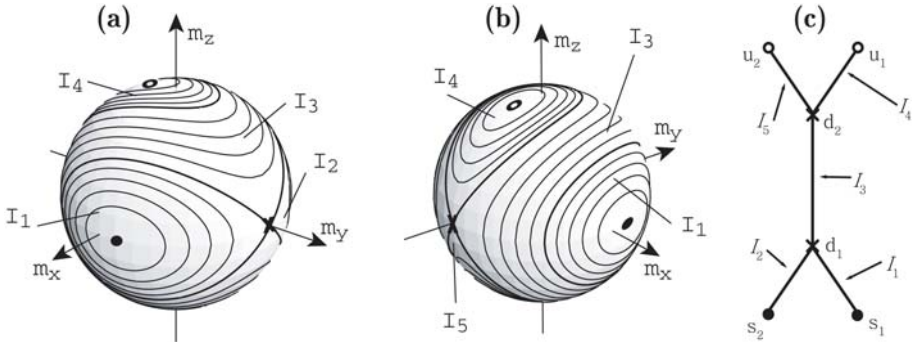

Fig. 1. (a, b) Magnetization trajectories of the conservative LLG dynamics on the unit sphere for $\mathbf{h}_a = h_{ay}\,\mathbf{e}_y$ and $0 < h_{ay} < D_z - D_y < D_y - D_x$. Filled dot: energy minimum; open dot: energy maximum; cross: energy saddle; bold lines: separatrices. System parameters: $D_x = -0.7$, $D_y = 0.3$, $D_z = 0.95$, $\mu_0 M_s = 1.76$ T, $h_{ay} = 0.2$. (c) Corresponding graph. s_1, s_2: energy minima; d_1, d_2: saddles; u_1, u_2: energy maxima. I_1, I_2, I_3, I_4, I_5: energy regions.

Since the injected current and the applied field are time independent, equation (1) (or equivalently Eq. (4)) describes an autonomous open dynamical system, forced far from equilibrium by the injected current, which evolves onto the surface of the unit sphere $|\mathbf{m}|^2 = 1$. The topological consequences of this fact are (Poincaré-Bendixson theorem [32]) that chaos is precluded and the only possible states reached by the magnetization are either stationary modes associated with static solutions (fixed points) of equation (1) or self-oscillations associated with periodic solutions (limit cycles) of equation (1). The key point is to determine these two types of magnetization response for different values of current and field [18].

In this respect a basic role is played by the fact that $\alpha \ll 1$ and $\beta \ll 1$. This implies that the dynamics described by equation (1) can be viewed as a perturbation of the conservative one, obtained by setting $\alpha = \beta = 0$ in equation (1): $d\mathbf{m}/dt = -\mathbf{m} \times \mathbf{h}_{\text{eff}}$ [18]. Therefore, a complete knowledge of the unperturbed dynamics is a necessary prerequisite in order to understand the non-conservative motions.

The conservative trajectories are closed curves given by the intersection between the unit sphere $|\mathbf{m}|^2 = 1$ and the energy surface $g_L(\mathbf{m}, \mathbf{h}_a) = g$ (see Eq. (2)), for various g and for fixed external field. Exact analytical solutions of this dynamics have been obtained when the external field is parallel to one of the principal axes of the energy surface [19,36]. In general, the conservative phase portrait may present six fixed points: two minima, two saddles, and two maxima. The trajectories passing through the saddles are called separatrices because they create a natural partition of the phase portrait into different energy regions (central regions), which are filled by a continuum of closed trajectories. In the most general case, five central regions are present in the phase portrait: two regions around energy minima, two regions around energy maxima, and one region between the two separatices which does not contain equilibria. In Figures 1a, 1b is shown an example of conservative phase portraits onto the surface of the $|\mathbf{m}|^2 = 1$ sphere, when $D_x < D_y < D_z$ and the external field, aligned to the y-axis, satisfies the condition $0 < h_{ay} < D_z - D_y < D_y - D_x$. Under increasing field, the number of fixed points is reduced from 6 to 4 and then to 2. In Figure 2a is shown an example of conservative phase portraits onto the surface of the $|\mathbf{m}|^2 = 1$ sphere where only 4 fixed points are present. In particular, the applied field is applied along the x-axis and satisfies the condition $D_y - D_x < h_{ax} < D_z - D_x$, with $D_x < D_y < D_z$.

A natural way to describe the topological properties of the conservative phase portrait is to specify an associated graph $\mathcal{G}$ [39]. In this graph, each edge represents a central region whereas each node corresponds to a saddle. We denote with I_k the kth central region (or graph edge) and with $[g_k^-, g_k^+]$ the corresponding interval for the energy g, that is, $\mathbf{m} \in I_k$ implies $g_k^- \leqslant g \leqslant g_k^+$. The conservative trajectory inside the kth central region for which $g_L(\mathbf{m}; \mathbf{h}_a) = g$ is indicated by $C_k(g)$. In this respect, we notice that each magnetization state $\mathbf{m}$ can be uniquely identified by specifying the value of the free energy $g = g_L(\mathbf{m}; \mathbf{h}_a)$, the index k of the branch of the graph $\mathcal{G}$ to which $\mathbf{m}$ belongs, and the position of $\mathbf{m}$ on the curve $C_k(g)$. The latter information can be given by introducing an azimuthal-like parameter ψ, assumed to vary in the interval $[0, 2\pi]$, which is used to give a parametric description of the curve $C_k(g)$. Examples of graphs are shown in Figures 1c and 2b, corresponding to the conservative phase portrait of Figures 1a, 1b and 2a, respectively.

On the basis of these general considerations, we go back to the study of the spin-torque driven magnetization dynamics. In particular, we determine the two types of magnetization response, that is, fixed points and limit cycles.

The fixed points $\mathbf{m}_0$ of the dynamics represent stationary magnetization states. They are calculated by setting $d\mathbf{m}_0/dt = 0$ into equation (1). Once the position of fixed points is obtained, we must determine their stability and calculate the bifurcation conditions which modify the number of fixed points (saddle-node bifurcations) or their stability (Hopf bifurcations) [32]. This kind of local bifurcations can be studied by linearizing equation (1) around each fixed point and by studying the corresponding stability matrix.

Limit cycles represent steady-state self-oscillations of the magnetization. The existence of this self-oscillatory

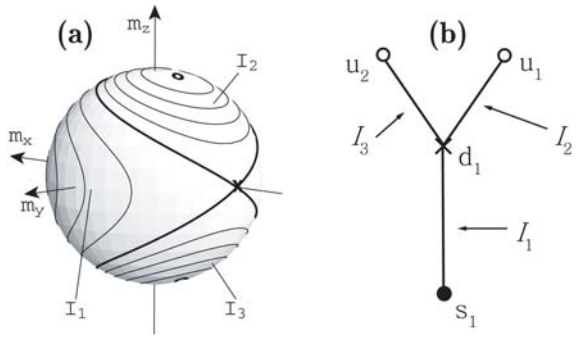

Fig. 2. (a) Magnetization trajectories of the conservative LLG dynamics on the unit sphere for $\mathbf{h}_a = h_{ax}\,\mathbf{e}_x$ and $D_y - D_x < h_{ax} < D_z - D_x$. Filled dot: energy minimum; open dot: energy maximum; cross: energy saddle; bold lines: separatrices. System parameters: $D_x = -0.034$, $D_y = 0$, $D_z = 0.68$, $\mu_0 M_s = 1.76$ T, $h_{ax} = 0.2$. (b) Corresponding graph. s_1: energy minimum; d_1: saddle; u_1, u_2: energy maxima. I_1, I_2, I_3: energy regions.

regime is related to the energy balance equation, obtained from equation (4):

$$\frac{dg_L}{dt} = -\alpha \left|\frac{d\mathbf{m}}{dt}\right|^2 - \beta \left(\mathbf{m} \times \frac{\partial \Phi_{ST}}{\partial \mathbf{m}}\right) \cdot \frac{d\mathbf{m}}{dt}. \qquad (5)$$

Equation (5) shows that the system free energy may increase or decrease during magnetization motion and under appropriate conditions the spin-torque contribution may provide energy to the system and counterbalance the damping process. If this occurs, the system can reach a steady periodic motion which we denote by $\mathbf{m}_p(t)$. In this case also $g_L(\mathbf{m}_p(t); \mathbf{h}_a)$ is periodic and so its derivative in time has zero average on one period. In other terms, a necessary condition for the existence of a periodic solution $\mathbf{m}_p(t)$ of equation (5) with period T_p is that:

$$\int_0^{T_p} \left(\alpha \left|\frac{d\mathbf{m}_p(t)}{dt}\right|^2 + \beta \frac{\mathbf{m}_p(t) \times \mathbf{e}_p}{1 + c_p \mathbf{m}_p(t) \cdot \mathbf{e}_p} \cdot \frac{d\mathbf{m}_p(t)}{dt} \right) dt = 0. \qquad (6)$$

This condition is quite evident from the physical point of view: periodic steady-state solutions require an average balance between loss and gain of energy. For slightly dissipative systems as the one described by equation (1), the periodic trajectory $\mathbf{m}_p(t)$ is close to a certain conservative trajectory $\mathbf{m}_k(t, g)$ of energy g. Thus no significant error is made if $\mathbf{m}_k(t, g)$ is used instead of $\mathbf{m}_p(t)$ in equation (6). Therefore, if we introduce the so-called Melnikov function $M_k(g, \mathbf{h}_a, \beta/\alpha)$:

$$M_k(g, \mathbf{h}_a, \beta/\alpha) = \int_0^{T_k(g)} \left(\left|\frac{d\mathbf{m}_k(t,g)}{dt}\right|^2 + \frac{\beta}{\alpha} \frac{\mathbf{m}_k(t,g) \times \mathbf{e}_p}{1 + c_p \mathbf{m}_k(t,g) \cdot \mathbf{e}_p} \cdot \frac{d\mathbf{m}_k(t,g)}{dt} \right) dt, \qquad (7)$$

where $T_k(g)$ is the period of the conservative trajectory, we expect that $M_k(g, \mathbf{h}_a, \beta/\alpha) \simeq 0$ for self-oscillations. These heuristic considerations can be given a rigorous form by making use of Poincaré-Melnikov theory [18,32] for slightly dissipative systems. This theory proves that the zeros of the Melnikov function correspond to limit cycles of the perturbed magnetization dynamics (Eq. (1)), provided α and β are small enough. These limit cycles are α-close to the conservative trajectory $C_k(g_{lc})$ corresponding to the value of energy g_{lc} for which the Melnikov function vanishes. More precisely, the Poincaré-Melnikov theory leads to the two fundamental results: (i) in the limit $\alpha \to 0$, $\beta \to 0$, $\beta/\alpha \to$ const., the equation $M_k(g_{lc}, \mathbf{h}_a, \beta/\alpha) = 0$ represents the necessary and sufficient condition for the existence of a periodic solution (limit cycle) of equation (1) inside the kth central energy region; (ii) the limit cycle is asymptotically coincident with the trajectory $C_k(g_{lc})$ of the conservative dynamics and is stable (unstable) when $\partial M_k(g_{lc}, \mathbf{h}_a, \beta/\alpha)/\partial g_{lc} > 0$ (< 0) [18]. Finally we notice that the Melnikov function vanishes at fixed points, that is, $M_k(g_{FP}, \mathbf{h}_a, \beta/\alpha) = 0$, where g_{FP} is the energy of a given fixed point.

Physically, $M_k(g, \mathbf{h}_a, \beta/\alpha)$ represents the rate of change of the system free energy averaged over one precessional period. It is worth remarking that we can transform the time integral appearing in equation (7) into a line integral along $C_k(g)$:

$$M_k(g, \mathbf{h}_a, \beta/\alpha) = \oint_{C_k(g)} \left(\mathbf{m} \times \frac{\partial \Phi}{\partial \mathbf{m}}\right) \cdot d\mathbf{m}, \qquad (8)$$

where:

$$\Phi(\mathbf{m}; \mathbf{h}_a, \beta/\alpha) = g_L(\mathbf{m}; \mathbf{h}_a) + \frac{\beta}{\alpha} \Phi_{ST}(\mathbf{m}). \qquad (9)$$

Therefore, the computation of $M_k(g, \mathbf{h}_a, \beta/\alpha)$ does not require the knowledge of the dependence of $\mathbf{m}_k(t, g)$ on time but only the geometric shape $C_k(g)$ of the trajectory on the unit sphere. The curve $C_k(g_{FP})$ reduces to a point when its corresponding energy equals the energy g_{FP} of a fixed point. Therefore, in this case the integral of equation (8) becomes identically zero and we obtain one more time that the Melnikov function vanishes at fixed points.

By making use of these results, it is possible to analytically construct the complete stability diagram, in the current-field control-plane, for spin-transfer-driven magnetization dynamics, since the Melnikov function provides all the information to determine the position of the bifurcations involving limit cycles, that is, Hopf, saddle-connection, and semi-stable limit-cycle bifurcations [32], [18]. In particular, we computed the stability diagram when the fixed-layer magnetization and the free-layer anisotropy are in-plane and the external field is parallel to the free-layer easy axis or perpendicular to the plane [18,19,33,34].

The Poincaré-Melnikov theory provides a method to predict the average energy associated with steady magnetization self-oscillations, but gives no information about the energy relaxation from any given initial condition and this final state. However, as a consequence of the fact that $\alpha \ll 1$ and $\beta \ll 1$, with ratio β/α of the order of unity, an approximate analytical approach can be followed to

obtained an equation which describes the time evolution of the energy. This approach is based on the fact that, due to the smallness of α and β, two widely different time scales are present in the dynamics: a fast one, over which precessional motion of the magnetization occurs, and a slow one, over which appreciable energy changes occur. This means that the magnetization executes many precessional oscillations before reaching the final state. Besides, in one precessional period the motion is very close to the conservative one. For this reason, no essential information on the energy evolution is lost if we take the average of equation (5) over one precessional period and we use the results obtained for the conservative dynamics to express the magnetization time dependence [35,36]. The result of this averaging is that the averaged energy follows the equation:

$$\frac{dg}{dt} = -\alpha \frac{M_k(g, \mathbf{h}_a, \beta/\alpha)}{T_k(g)}, \tag{10}$$

where $M_k(g, \mathbf{h}_a, \beta/\alpha)$ is precisely the Melnikov function previously introduced and $T_k(g)$ represents the period of the conservative motion of energy g inside the kth energy region. Equation (10) can be rewritten in the form:

$$\frac{dg}{dt} = -\alpha \frac{\partial U_k}{\partial g}, \tag{11}$$

where we have introduced the effective potential $U_k(g)$ defined, up to a constant, as:

$$U_k(g) = \int_{g_k^-}^{g} \frac{M_k(u, \mathbf{h}_a, \beta/\alpha)}{T_k(u)} du. \tag{12}$$

Equation (11) shows that, to the first order in α, the energy follows a viscous-like dynamics governed by the effective potential $U_k(g)$. This approximate description will be the more accurate, the smaller α, or, equivalently, the faster the magnetization precession with respect to the energy relaxation characteristic time. In particular, this description fails when we consider trajectories close to one of the separatrices, since in this case the trajectory period tends to infinity. Finally, we notice that the extrema of U_k, given by $\partial U_k/\partial g = 0$, correspond to fixed points and limit cycles of the complete dynamics, as result from the Poincaré-Melnikov theory. More precisely, $dU_k^2/dg^2 = (dM_k/dg)/T_k(g)$ when calculated for energy values corresponding to limit cycles or fixed points. On the other hand, $dM_k/dg > 0$ for stable states and $dM_k/dg < 0$ for unstable ones. Therefore, minima and maxima of U_k correspond to stable and unstable steady states, respectively.

3 Effect of thermal fluctuations

The analytical predictions discussed in the previous section were obtained without taking into account the role of temperature. To describe the effect of thermal fluctuations on spin-torque-driven magnetization dynamics, we follow an approach inspired by Brown's one [23] for the treatment of thermal switching in fine particles. The basis of this approach is to add a random magnetic torque to the LLG equation and to study the ensuing stochastic magnetization dynamics. The separation of time scales leading to equation (10) for the deterministic dynamics is also a property of the stochastic dynamics. This permits one to derive a relaxation-diffusion equation for the energy and to identify the effective potential analogous to $U_k(g)$ in equation (11) which controls the thermal fluctuations of the system around a steady state and the transition probabilities from one steady state to another consequent to thermal effects.

As first step, we rewrite equation (4) in a form explicit with respect to $d\mathbf{m}/dt$. Since α and β are small quantities, one can approximate this equation to the first order in α and β, obtaining:

$$\frac{d\mathbf{m}}{dt} = \mathbf{m} \times \frac{\partial g_L}{\partial \mathbf{m}} + \alpha\, \mathbf{m} \times \left(\mathbf{m} \times \frac{\partial \Phi}{\partial \mathbf{m}} \right), \tag{13}$$

where Φ is given by equation (9). Then we add the random magnetic torque $-\nu \mathbf{m} \times \mathbf{h}_N(t)$, where $\mathbf{h}_N(t)$ represents Gaussian white noise, that is, $\mathbf{h}_N(t)dt = d\mathbf{W}$, where $d\mathbf{W}$ represents the increment of the standard isotropic vector Wiener process $\mathbf{W}(t)$, with $\langle |dW_i|^2 \rangle = dt$ $(i = x, y, z)$. The intensity of thermal effects is measured by the parameter ν [37]. Therefore we obtain:

$$\frac{d\mathbf{m}}{dt} = \mathbf{m} \times \frac{\partial g_L}{\partial \mathbf{m}} + \alpha\, \mathbf{m} \times \left(\mathbf{m} \times \frac{\partial \Phi}{\partial \mathbf{m}} \right) - \nu \mathbf{m} \times \mathbf{h}_N(t). \tag{14}$$

By interpreting this Langevin equation (14) in the sense of Stratonovich [37,38] we can apply the ordinary rules of calculus [37] to obtain $d|\mathbf{m}|^2/dt = \mathbf{m} \cdot d\mathbf{m}/dt = 0$. Thus, the magnetization magnitude is still conserved and the magnetization motion keeps on taking place onto the surface of the unit sphere $|\mathbf{m}|^2 = 1$, as for the deterministic dynamics. The associated Fokker-Planck for the probability density $W(\mathbf{m}, t)$ is [37]:

$$\frac{\partial W(\mathbf{m}, t)}{\partial t} = -\mathrm{div}_{\Sigma} \mathbf{J}, \tag{15}$$

where the symbol div_{Σ} represents the divergence operator acting on the surface Σ of the unit sphere. The probability current is given by:

$$\mathbf{J} = (\mathbf{m} \times \nabla_{\Sigma} g_L - \alpha \nabla_{\Sigma} \Phi) W - \frac{\nu^2}{2} \nabla_{\Sigma} W, \tag{16}$$

where the symbol ∇_{Σ} represents the gradient operator acting on Σ. The value of the constant ν is obtained from the fluctuation-dissipation theorem in the thermodynamics equilibrium, corresponding to the case of $\beta = 0$:

$$\nu^2 = \frac{2\alpha k_B T}{\mu_0 M_s^2 V}, \tag{17}$$

where V is the volume of the nanomagnet. For the following analysis we will assume that the damping constant α

as well as the statistical properties of the noise term in equation (4), and in particular the value of ν expressed by equation (17), are not affected by the injection of the current. In the sequel we will also use the notation $\mu = 2\alpha/\nu^2$.

In order to study the Fokker-Planck equation (see Eqs. (15–17)) in the limit of small fluctuations and small nonconservative effects ($\alpha \ll 1$, $\nu \sim \sqrt{\alpha}$), and thus to take advantage of the fact that stochastic magnetization dynamics given by equation (14) is a perturbation of conservative dynamics, it is convenient to use a coordinate system on the unit sphere in which energy is one of the coordinate variables. We introduce the unit vectors:

$$\mathbf{e}_g = \frac{\nabla_\Sigma g_L}{|\nabla_\Sigma g_L|}\ ,\ \ \mathbf{e}_\psi = \mathbf{m} \times \mathbf{e}_g, \tag{18}$$

orthogonal and tangential to the line $C_k(g)$, respectively. The differential displacements (dm_g, dm_ψ) of $\mathbf{m}$ along $\mathbf{e}_g$ and $\mathbf{e}_\psi$, associated with infinitesimal changes $(dg, d\psi)$ of the coordinates, are respectively given by:

$$dm_g = \mathbf{e}_g \cdot d\mathbf{m} = l_g dg\,, \quad dm_\psi = \mathbf{e}_\psi \cdot d\mathbf{m} = l_\psi d\psi, \tag{19}$$

where l_g and l_ψ are appropriate "metric factors". From equation (18) one finds that:

$$l_g = 1/|\nabla_\Sigma g_L|. \tag{20}$$

By using this coordinate system we can rewrite equations (15) and (16) in terms of the the coordinates (g, ψ) and of the index k labeling the energy region to which (g, ψ) refer:

$$\frac{\partial \rho_k}{\partial t} = -\frac{\partial}{\partial g}\left(l_\psi J_{k,g}\right) - \frac{\partial}{\partial \psi}\left(l_g J_{k,\psi}\right), \tag{21}$$

where:

$$\rho_k(g, \psi, t) = W_k(g, \psi, t)\, l_g l_\psi \tag{22}$$

is the probability density as a function of (g, ψ), $W_k(g, \psi, t)$ is the function $W(\mathbf{m}, t)$ after $\mathbf{m}$ is expressed in the new coordinates (g, ψ), whereas:

$$J_{k,g} = \mathbf{J} \cdot \mathbf{e}_g = -\alpha \frac{W_k}{l_g}\frac{\partial \Phi}{\partial g} - \frac{\nu^2}{2}\frac{1}{l_g}\frac{\partial W_k}{\partial g} \tag{23}$$

and

$$J_{k,\psi} = \mathbf{J} \cdot \mathbf{e}_\psi = \frac{W_k}{l_g} - \alpha W_k \frac{1}{l_\psi}\frac{\partial \Phi}{\partial \psi} - \frac{\nu^2}{2}\frac{1}{l_\psi}\frac{\partial W_k}{\partial \psi} \tag{24}$$

are the probability currents along $\mathbf{e}_g$ and $\mathbf{e}_\psi$, respectively. In this formalism the Melnikov function (Eq. (8)) takes the form:

$$M_k(g, \mathbf{h}_a, \beta/\alpha) = \oint_{C_k(g)} \frac{1}{l_g}\frac{\partial \Phi}{\partial g} dm_\psi, \tag{25}$$

$$M_k^0(g, \mathbf{h}_a) = \oint_{C_k(g)} |\nabla_\Sigma g| dm_\psi, \tag{26}$$

where $M_k^0(g, \mathbf{h}_a) = M_k(g, \mathbf{h}_a, \beta/\alpha = 0)$. The probability densities $\rho_k(g, \psi, t)$ and $W_k(g, \psi, t)$ satisfy the following normalization conditions:

$$\sum_k \int_{I_k} \int_0^{2\pi} \rho_k(g, \psi, t) dg d\psi = 1, \tag{27}$$

$$\sum_k \int_{I_k} \int_0^{2\pi} W_k(g, \psi, t) l_g l_\psi dg d\psi = 1. \tag{28}$$

Two time scales are present in the Fokker-Planck equation (Eqs. (21, 24)), which are well-separated when α and ν^2 ($\sim\alpha$) are small parameters: a fast time scale connected to the fast precessional drift and described by the first term in the probability current $J_{k,\psi}$ (Eq. (24)), and a slow time scale connected to slow relaxation and diffusion, described by all other terms (which are proportional to α), in equations (23) and (24). The existence of two distinct time scales can be used to derive an approximate description of the diffusion process based on the averaging technique. This idea has been already applied to the deterministic magnetization dynamics at the end of the previous section. The starting point for the averaging analysis is to write the probability density $\rho_k(g, \psi, t)$ as:

$$\rho_k(g, \psi, t) = \rho_k(\psi, t|g)\rho_k(g, t), \tag{29}$$

where $\rho_k(\psi, t|g)$ is the conditional probability density under given energy and:

$$\rho_k(g, t) = \int_0^{2\pi} \rho_k(g, \psi, t) d\psi. \tag{30}$$

By taking into account equations (19, 20), and (22), equation (30) can be written in the line-integral form:

$$\rho_k(g, t) = \oint_{C_k(g)} \frac{W(\mathbf{m}, t)}{|\nabla_\Sigma g_L|} dm_\psi. \tag{31}$$

In the limit of small α, the energy remains practically constant for a large number of periods of oscillation and appreciable time variations of $\rho_k(g, t)$ are expected to occur only on a time scale of the order of $1/\alpha$. This scale is suggested by the fact that $J_{k,g}$ is proportional to α. In fact, by integrating equation (21) with respect to ψ in the interval $[0, 2\pi]$ and taking into account the periodicity of all quantities with respect to ψ, one obtains that $\partial\rho_k(g, t)/\partial t$ is first-order in α. On the other hand, the conditional distribution $\rho_k(\psi, t|g)$ has a fast time variation regardless of the smallness of α, that is, $\partial\rho_k(\psi, t|g)/\partial t$ is zeroth-order with respect to α. According to the above discussion, the key assumption of the averaging method is that the conditional probability distribution $\rho_k(\psi, t|g)$ reaches equilibrium on the short time scale well before any appreciable change in $\rho_k(g, t)$ takes place [40]. Thus, in the long time scale, $\rho_k(g, \psi, t)$ takes the form:

$$\rho_k(g, \psi, t) = \rho_k^{eq}(\psi|g)\rho_k(g, t) + \mathcal{O}(\alpha), \tag{32}$$

where $\rho_k^{eq}(\psi|g)$ is the distribution obtained when $\rho_k(\psi, t|g)$ reaches equilibrium. This equilibrium conditional probability can be found by computing the time derivative of

equation (29), substituting it in equation (21), and considering only the zeroth-order terms with respect to α. In this way, we obtain the equation:

$$\frac{\partial}{\partial t}\rho_k(\psi,t|g) = \frac{\partial}{\partial \psi}\left(\frac{\rho_k(\psi,t|g)}{l_g l_\psi}\right). \tag{33}$$

The stationary solution $\rho_k^{eq}(\psi|g)$ fulfills the equation:

$$\frac{\partial}{\partial \psi}\left(\frac{\rho_k^{eq}(\psi|g)}{l_g l_\psi}\right) = 0, \tag{34}$$

whose solution is:

$$\rho_k^{eq}(\psi|g) = c_k(g) l_g l_\psi, \tag{35}$$

where $c_k(g)$ is a function of energy to be determined by the normalization condition:

$$\int_0^{2\pi} \rho_k^{eq}(\psi|g)d\psi = 1. \tag{36}$$

By using equations (19, 20, 35), and (36), one finds $c_k(g) = 1/T_k(g)$, that is:

$$\rho_k^{eq}(\psi|g) = \frac{l_g l_\psi}{T_k(g)}, \tag{37}$$

where

$$T_k(g) = \oint_{C_k(g)} \frac{dm_\psi}{|\nabla_\Sigma g_L|}, \tag{38}$$

is the period of the conservative precessional motion along the trajectory $C_k(g)$. One can verify that the equilibrium conditional probability density, given by equation (37) is inversely proportional to the velocity of magnetization precession along $C_k(g)$.

Equations (22, 32), and (37) imply that in the averaging approximation $W_k(g,\psi,t)$ is in fact virtually independent of ψ on the long time scale:

$$W_k(g,\psi,t) = \frac{\rho_k(g,t)}{T_k(g)} + \mathcal{O}(\alpha). \tag{39}$$

We will denote the dominant part by $W_k(g,t)$:

$$W_k(g,t) = \frac{\rho_k(g,t)}{T_k(g)}. \tag{40}$$

By substituting equations (32, 37), and (39) into equation (21), neglecting all second-order terms in α, integrating with respect to ψ on $[0,2\pi]$, one obtains the averaged Fokker-Planck equation:

$$\frac{\partial \rho_k(g,t)}{\partial t} = -\frac{\partial J_k(g)}{\partial g}, \tag{41}$$

where:

$$J_k(g) = \oint_{C_k(g)} J_{k,g}\, dm_\psi. \tag{42}$$

In terms of $W_k(g,t)$, equations (41) and (42) read:

$$T_k(g)\frac{\partial W_k(g,t)}{\partial t} = -\frac{\partial J_k(g)}{\partial g}, \tag{43}$$

$$J_k(g) = -M_k^0(g,\mathbf{h}_a)\left(\alpha\frac{M_k(g,\mathbf{h}_a,\beta/\alpha)}{M_k^0(g,\mathbf{h}_a)}W_k + \frac{\nu^2}{2}\frac{\partial W_k}{\partial g}\right), \tag{44}$$

where $M_k(g,\mathbf{h}_a,\beta/\alpha)$ and $M_k^0(g,\mathbf{h}_a)$ are the Melnikov functions defined by equations (25) and (26), while $W_k(g,t)$ fulfills the normalization condition:

$$\sum_k \int_{I_k} T_k(g) W_k(g,t) dg = 1. \tag{45}$$

Equations (43) and (44) have to be solved on the graph $\mathcal{G}$. In this respect, boundary conditions at the graph nodes are required for the probability distribution and the probability current [41]. In particular, $W_k(g,t)$ must be continuous on the graph and the sum of all the incoming probability currents must be zero at each node of the graph.

To study equation (43) we first rewrite the probability current J_k in a more useful form by introducing the function:

$$V_k(g) = \int_{g_k^-}^{g} \frac{M_k(u,\mathbf{h}_a,\beta/\alpha)}{M_k^0(u,\mathbf{h}_a)}du + d_k, \tag{46}$$

where d_k is an arbitrary integrating factor which must be determined by imposing that $V_k(g)$ is continuous on the graph $\mathcal{G}$. For example, in the case considered in Figure 2, $V_1(g_d) = V_2(g_d) = V_3(g_d)$, where g_d is the value of the energy at the saddle d_1. In order to simplify the derivation of the stationary distribution function we multiply both sides of equation (44) by the integrating factor $\exp(\mu V_k(g))$. We obtain:

$$J_k(g) = -\frac{\nu^2}{2}M_k^0(g,\mathbf{h}_a)e^{-\mu V_k(g)}\frac{\partial}{\partial g}\left[e^{\mu V_k(g)}W_k\right], \tag{47}$$

where $\mu = 2\alpha/\nu^2$. In this manner, the stationary distribution function $W_k^{eq}(g)$ can be immediately derived by imposing $J_k(g) = 0$ into equation (47) and by satisfying the boundary and normalization conditions. The result is:

$$W_k^{eq}(g) = \frac{1}{Z(\mu)}e^{-\mu V_k(g)}, \tag{48}$$

where:

$$Z(\mu) = \sum_k \int_{I_k} e^{-\mu V_k(g)} T_k(g) dg. \tag{49}$$

The expression of $W_k^{eq}(g)$ (Eq. (48)) is formally coincident with the usual Boltzmann distribution, where $Z(\mu)$ and $V_k(g)$ play the role of partition function and potential energy, respectively. However, $W_k^{eq}(g)$ is not an equilibrium distribution in the statistical mechanical sense but rather a stationary out-of-equilibrium distribution induced by the spin-polarized current and, as such, dependent on β/α.

The function $V_k(g)$ has to be considered an "effective potential" which governs the stochastic dynamics, as shown in equation (48). The role of $V_k(g)$ in the dynamics of the system is better appreciated by comparing it with the potential $U_k(g)$ introduced for the deterministic dynamics (see Eq. (12)). By comparing equation (12) to

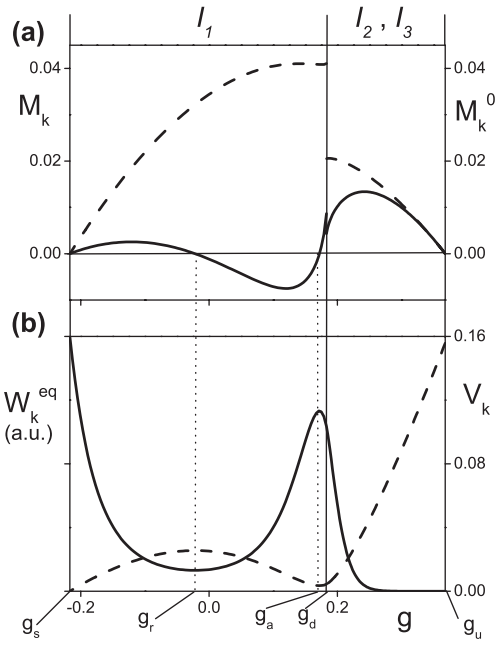

Fig. 3. (a) Melnikov functions M_k (bold line) and M_k^0 (dashed line) corresponding to energy regions I_k of Figure 2. (b) Stationary probability distribution W_k^{eq} (bold line) and corresponding effective potential V_k (dashed line). g_s: energy minimum; g_r: energy of unstable limit cycle; g_a: energy of stable limit cycle; g_d: energy saddle; g_u: energy maximum. $[g_s, g_d]$ is the energy interval associated with I_1, $[g_d, g_u]$ is that associated with I_2 and I_3. System parameters: $D_x = -0.034$, $D_y = 0$, $D_z = 0.68$, $\alpha = 0.014$, $P = 0.3$, $V = 5\,10^{-25}$ m^3, $\mu_0 M_s = 1.76$ T, $T = 300$ K, $\mathbf{h}_a = 0.2\mathbf{e}_x$, $\beta/\alpha = 0.675$.

equation (46) we find that these two potentials are connected by the following equation:

$$\frac{\partial V_k}{\partial g} = \frac{T_k}{M_k^0}\frac{\partial U_k}{\partial g}. \tag{50}$$

Since both M_k^0 and T_k are positive-definite quantities, V_k and U_k exhibit the same distribution of maxima and minima. Therefore, according to equation (48) and the analysis on U_k discussed at the end of the previous section, the stationary distribution function W_k^{eq} is peaked around the stable states of the deterministic dynamics. An example of V_k and W_k^{eq} is shown in Figure 3, whereas in Figure 4 we show how V_k and W_k^{eq} change when the current is increased under fixed external field.

Equation (50) shows that the generalized driving forces associated with the potentials U_k and V_k are different. The consequence of this fact is that the stochastic equation for the energy cannot be obtained by simply adding a noise term to equation (10). This can be shown by first writing the Fokker-Planck equation for $\rho_k(g,t)$ (Eq. (41)), which is the probability density with respect to g. By making

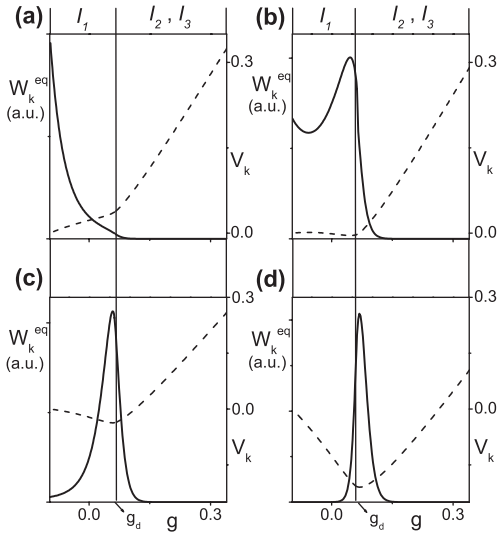

Fig. 4. Evolution of W_k^{eq} (bold lines) and V_k (dashed lines) for increasing current and fixed external field. Energy intervals corresponding to $I_k (k = 1, 2, 3)$ are indicated. System parameters: $D_x = -0.034$, $D_y = 0$, $D_z = 0.68$, $\alpha = 0.014$, $P = 0.3$, $V = 5\,10^{-25}$ m^3, $\mu_0 M_s = 1.76$ T, $T = 300$ K, $\mathbf{h}_a = 0.08\mathbf{e}_x$. g_d: energy saddle. (a): $\beta/\alpha = 0.5$; (b): $\beta/\alpha = 0.66$; (c): $\beta/\alpha = 0.8$; (d): $\beta/\alpha = 1.5$. These system parameters correspond to those considered in the case of Figure 3 in [18].

use of equation (39) we obtain:

$$\frac{\partial \rho_k(g,t)}{\partial t} = \frac{\partial}{\partial g}\left[\left(\alpha\frac{M_k(g)}{T_k(g)} - \frac{\nu^2}{2T_k(g)}\frac{dM_k^0(g)}{dg}\right)\rho_k(g,t)\right] + \frac{\nu^2}{2}\frac{\partial^2}{\partial g^2}\left(\frac{M_k^0(g)}{T_k(g)}\rho_k(g,t)\right) \tag{51}$$

(dependencies on $\mathbf{h}_a$ and β/α are understood). According to the theory of stochastic processes [37], to equation (51) there corresponds the Ito stochastic differential equation for g:

$$\frac{dg}{dt} = -\left(\alpha\frac{M_k(g)}{T_k(g)} - \frac{\nu^2}{2T_k(g)}\frac{dM_k^0(g)}{dg}\right) + \nu\sqrt{\frac{M_k^0(g)}{T_k(g)}}h_N(t), \tag{52}$$

where $h_N(t)$ represents Gaussian white noise [39]. In the limit $\nu \to 0$, equation (52) reduces to equation (10) for the deterministic dynamics. On the other hand, when $\nu \neq 0$, an additional drift term appears in the relaxation process for g. This term can only be revealed by the rigorous analytical treatment previously discussed which involves the Fokker-Planck equation associated with the diffusion process on the unit sphere.

Through the effective potential $V_k(g)$, one can introduce the concept of potential barrier separating a stable fixed point and a limit cycle, although there is no potential barrier in terms of the free energy g_L. As previously discussed, since stable and unstable states of the deterministic dynamics respectively correspond to minima and maxima of $V_k(g)$, it is natural to define the potential barrier ΔV_k as:

$$\Delta V_k = V_k(g_{max}) - V_k(g_{min}), \tag{53}$$

where g_{max} and g_{min} denote the energy values for the maximum and minimum of $V(g)$, respectively. For example, if the system shows an unstable limit cycle between a stable limit cycle and a stable fixed point in the energy region I_k, the potential barrier which has to be overcome to exit the basin of attraction around the stable point is given by $V_k(g_r) - V_k(g_s)$, whereas the potential barrier which has to be overcome to exit the basin of attraction around the stable limit cycle is $V_k(g_r) - V_k(g_a)$, where g_s, g_a, and g_r denote the energy values of the stable fixed point, the stable limit cycle, and the unstable limit cycle, respectively. An example of this situation is shown in Figure 3. Since the energy values corresponding to limit cycles depend on the injected current through the equations $M_k(g_a, \mathbf{h}_a, \beta/\alpha) = 0$ and $M_k(g_r, \mathbf{h}_a, \beta/\alpha) = 0$, the potential barriers $V_k(g_r) - V_k(g_s)$ and $V_k(g_r) - V_k(g_a)$ depend on the injected current through a nontrivial relationship. However, if we are interested in the transition from a stable fixed point to a stable state in another energy region, the potential barrier to be overcome is $V_k(g_d) - V_k(g_s)$, where g_d is the energy value of the saddle, which is current independent. By applying equation (46) to this case we obtain:

$$V_1(g_d) - V_1(g_s) = (g_d - g_s)\,(1 - J_e/J_c), \tag{54}$$

where J_c is a constant with the dimensions of an electric density current. Equation (54) shows that in this case the potential barrier is linearly dependent on injected current.

In the limit of "high-energy barrier" approximation, that is, $\mu\Delta V_k \gg 1$, one can follow the approach introduced by Brown [23] to compute the transition rate from a basin of attraction to another [30]. An example will be discussed in the next section.

4 Uniaxial symmetry

The results discussed in the previous sections acquire a particularly simple form for systems exhibiting uniaxial symmetry, that is, systems characterized by the fact that the free-layer easy axis, the fixed-layer easy axis, and the external magnetic field directions are all along the z axis perpendicular to the layer plane, while the layer properties show uniaxial symmetry around that axis. In particular, one has that $D_x = D_y = D_\perp$. Systems with this type of symmetry are of great pedagogical interest and are also under consideration for possible applications in data-storage [42].

Thanks to the rotational symmetry around the z-axis, the LLG equation with Slonczewski spin-transfer term takes a simpler form and the deterministic dynamics can be solved in full detail. The effective field takes the expression $\mathbf{h}_{\text{eff}} = [h_{az} - (D_z - D_\perp)m_z]\,\mathbf{e}_z$ and an independent equation for the magnetization component along the z axis exists. From equation (4) one obtains:

$$\frac{dm_z}{dt} = -\alpha\frac{\partial \Phi}{\partial m_z}(1 - m_z^2), \tag{55}$$

where it has been taken into account that in this case $\mathbf{e}_p \equiv \mathbf{e}_z$. It is useful to describe the system in terms of spherical coordinates (θ, ϕ), that is, $m_x = \sin\theta\cos\phi$, $m_y = \sin\theta\sin\phi$, $m_z = \cos\theta$. In terms of θ, equation (55) takes the following form:

$$\frac{d\theta}{dt} = -\alpha\frac{\partial \Phi}{\partial \theta}. \tag{56}$$

It is clear from equation (56) that the function Φ acts as an effective potential governing the dynamics of the polar angle θ. Φ depends on θ only:

$$\begin{aligned}\Phi(\theta; h_{az}, \beta/\alpha) &= g_L(\theta; h_{az}) + \frac{\beta}{\alpha}\Phi_{ST}(\theta)\\ &= \frac{1}{2}(D_z - D_\perp)\cos^2\theta - h_{az}\cos\theta + \frac{\beta}{\alpha}\frac{1}{c_p}\ln(1 + c_p\cos\theta),\end{aligned} \tag{57}$$

where h_{az} is the intensity of the field applied along the z axis. From equation (56) we have that fixed points and limit cycles of the dynamics are all solutions of the equation $\partial\Phi/\partial\theta = 0$ under the constraint $|\cos\theta| \leqslant 1$. In particular, only two fixed points, $\theta = 0$ and $\theta = \pi$, exist and they are always present, for all values of field and injected current. Other solutions of $\partial\Phi/\partial\theta = 0$ for $\theta \neq 0$ and $\theta \neq \pi$ represent limit cycles in which the magnetization precesses around the symmetry axis. The fixed points and limit cycles are stable if $\partial^2\Phi/\partial\theta^2 > 0$ and unstable if $\partial^2\Phi/\partial\theta^2 < 0$. This means that stable fixed points and limit cycles are minima of the function Φ. Besides, according to the stability diagram discussed in [17], $h_{az} \approx (D_z - D_\perp)/c_p$ and $\beta/\alpha \approx (1 - c_p^2)(D_z - D_\perp)/c_p$ are the values of field and current around which limit cycles, that is, self-oscillation regimes, may exist in the dynamics. Figure 5 shows examples of the behavior of Φ for different values of the injected current.

In order to study the effect of thermal fluctuations, we can write the Fokker-Planck equation (Eqs. (15) and (16)) in spherical coordinates (θ, ϕ):

$$\frac{\partial W(\theta, \phi, t)}{\partial t} = -\frac{1}{\sin\theta}\frac{\partial}{\partial\theta}(\sin\theta J_\theta) - \frac{1}{\sin\theta}\frac{\partial J_\phi}{\partial\phi}, \tag{58}$$

where:

$$J_\theta = -\frac{W}{\sin\theta}\frac{\partial g_L}{\partial\phi} - \alpha W\frac{\partial\Phi}{\partial\theta} - \frac{\nu^2}{2}\frac{\partial W}{\partial\theta} \tag{59}$$

$$J_\phi = W\frac{\partial g_L}{\partial\theta} - \frac{\alpha W}{\sin\theta}\frac{\partial\Phi}{\partial\phi} - \frac{\nu^2}{2\sin\theta}\frac{\partial W}{\partial\phi}. \tag{60}$$

By integrating equation (58) over ϕ and by taking into account that g_L and Φ are independent of ϕ because of symmetry, one obtains the equation:

$$\frac{\partial\overline{P}}{\partial t} = \frac{\partial}{\partial\theta}\left[\left(\alpha\frac{\partial\Phi}{\partial\theta} - \frac{\nu^2}{2}\cot\theta\right)\overline{P} + \frac{\nu^2}{2}\frac{\partial\overline{P}}{\partial\theta}\right], \tag{61}$$

where $\overline{P} = \sin\theta\int_0^{2\pi} W(\theta, \phi, t)d\phi$ represents the probability density with respect to θ. This Fokker-Planck equation corresponds to the following Langevin-type equation for θ:

$$\frac{d\theta}{dt} = -\alpha\frac{\partial\Phi}{\partial\theta} + \frac{\nu^2}{2}\cot\theta + \nu h_N(t), \tag{62}$$

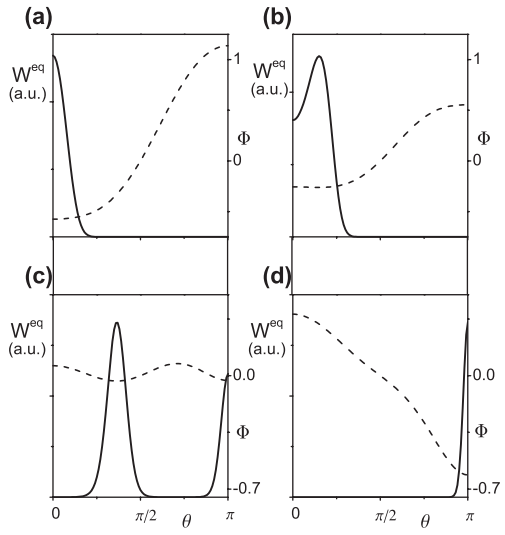

Fig. 5. Evolution of W^{eq} (bold line) and Φ (dashed line) for increasing current and fixed external field. System parameters: $D_z = 1$, $D_\perp = 0$, $\alpha = 0.01$, $P = 0.3$, $V = 5\,10^{-25}$ m^3, $\mu_0 M_s = 1$ T, $T = 300$ K, $h_{az} = 1.6$. (a): $\beta/\alpha = 0.66$; (b): $\beta/\alpha = 1.06$; (c): $\beta/\alpha = 1.46$; (d): $\beta/\alpha = 1.86$.

where $h_N(t)$ represents Gaussian white noise. Equation (62), as equation (52), shows an additional drift term related to the description of the state in terms of θ.

For uniaxial systems, the vector fields $\nabla_\Sigma g_L$ and $\nabla_\Sigma \Phi$ present in equation (16) are parallel everywhere, as a consequence of the rotational symmetry of the problem. This leads to the following expression for the stationary distribution function:

$$W^{eq}(\theta) = \frac{1}{Z(h_{az}, \beta/\alpha)}\, e^{-\mu\Phi(\theta)}. \qquad (63)$$

We remind that equation (63), as equation (48), despite its Boltzmann form, does not correspond to equilibrium, but rather to stationary out-of-equilibrium condition dependent on β/α. An example of the behavior of W^{eq} for different current values is given in Figure 5.

In the particular case of Figure 5c, $\theta = \pi$ is stable but $\theta = 0$ is not, which means that, despite the substantial positive effective field $\mathbf{h}_{\text{eff}} = h_{az} - (D_z - D_\perp) = 0.6$ acting on the nanomagnet, the effect of the current is strong enough to destroy the stability of the $\theta = 0$ state. Two limit cycles exist for $\theta_0 \simeq 1.15$ and $\theta_0 \simeq 2.23$, of which the former is stable and the latter unstable. The barrier $\Delta\Phi$ separating these two stable states is $\Delta\Phi \approx 0.1$, corresponding to an energy barrier of the order of 10 $k_B T$ for $V = 5 \times 10^{-25}$ m^3, $\mu_0 M_s = 1$ T, and $T = 300$ K.

Some remarks can be made at this point. First, we observe that, thanks to uniaxial symmetry, the approximations discussed in the previous section, involving the separation of two time scales, are not required to derive equations (61–63). Second, since g_L and Φ depend on θ only, the angle θ describes both the magnetization state and the energy state of the system. By making explicit the θ dependence in $V_k(g(\theta))$ (Eq. (46)) one finds that $\Phi(\theta) = V_k(g(\theta))$. Therefore, in this case, both the deterministic and the stochastic dynamics are governed by the same potential $\Phi(\theta)$, as we can observe from equations (56) and (63). Finally, one can derive expressions for the transition rate $1/\tau_{ij}$ from a stable state (θ_i) to another one (θ_j) by following the approach discussed by Brown in [23]. One finds:

$$\frac{1}{\tau_{ij}} = \alpha k_i \sin\theta_m \sqrt{\frac{\alpha k_m}{\pi\nu^2}}\, e^{-\mu(\Phi(\theta_m) - \Phi(\theta_i))}, \qquad (64)$$

where θ_m denotes the maximum of Φ included between θ_i and θ_j, $k_i = \Phi''(\theta_i)$, and $k_m = -\Phi''(\theta_m)$. By considering the case of Figure 5(c), the two stable states are $\theta_1 \simeq 1.15$ and $\theta_2 = \pi$, whereas the maximum between them corresponds to the unstable limit cycle for $\theta_m \simeq 2.23$. In physical units, the frequencies of transition are $f_{12} \approx 40$ kHz and $f_{21} \approx 100$ kHz.

References

1. L. Berger, Phys. Rev. B **54**, 9353 (1996)
2. J.C. Slonczewski, J. Magn. Magn. Mater. **159**, L1 (1996)
3. M. Tsoi, A.G.M. Jansen, J. Bass, W.C. Chiang, M. Seck, V. Tsoi, P. Wyder, Phys. Rev. Lett. **80**, 4281 (1998)
4. E.B. Myers, D.C. Ralph, J.A. Katine, R.N. Louie, R.A. Buhrman, Science **285**, 867 (1999)
5. J.A. Katine, F.J. Albert, R.A. Buhrman, E.B. Myers, D.C. Ralph, Phys. Rev. Lett. **84**, 3149 (2000)
6. S.I. Kiselev, J.C. Sankey, I.N. Krivorotov, N.C. Emley, R.J. Schoelkopf, R.A. Buhrman, D.C. Ralph, Nature **425**, 380 (2003)
7. W.H. Rippard, M.R. Pufall, S. Kaka, S.E. Russek, T.J. Silva, Phys. Rev. Lett. **92**, 027201 (2004)
8. C. Heide, Phys. Rev. B **65**, 054401 (2002)
9. M.D. Stiles, A. Zangwill, Phys. Rev. B **66**, 014407 (2002)
10. S. Zhang, P.M. Levy, A. Fert, Phys. Rev. Lett. **88**, 236601 (2002)
11. J.C. Slonczewski, J. Magn. Magn. Mater. **195**, L261 (1999)
12. A.N. Slavin, V.S. Tiberkevich, Phys. Rev. B **72**, 094428 (2005)
13. S.M. Rezende, F.M. de Aguiar, A. Azevedo, Phys. Rev. Lett. **94**, 037202 (2005)
14. J. Miltat, G. Albuquerque, A. Thiaville, C. Vouille, J. Appl. Phys. **89**, 6982 (2001)
15. Z. Li, S. Zhang, Phys. Rev. B **68**, 024404 (2003)
16. D. Berkov, N. Gorn, Phys. Rev. B **71**, 052403 (2005)
17. Y.B. Bazaliy, B.A. Jones, S.C. Zhang, Phys. Rev. B **69**, 094421 (2004)
18. G. Bertotti, C. Serpico, I.D. Mayergoyz, A. Magni, M. d'Aquino, R. Bonin, Phys. Rev. Lett. **94**, 127206 (2005)
19. G. Bertotti, I.D. Mayergoyz, C. Serpico, in *The Science of Hysteresis. Volume II: Physical Modeling, Micromagnetics, and Magnetization Dynamics*, edited by G. Bertotti, I.D. Mayergoyz (Elsevier, Oxford, 2006), p. 435
20. S. Urazhdin, N.O. Birge, W.P. Pratt, J. Bass, Phys. Rev. Lett. **91**, 146803 (2003)
21. A. Fabian, C. Terrier, S. Serrano-Guisan, X. Hoffer, M. Dubey, L. Gravier, J.P. Ansermet, Phys. Rev. Lett. **91**, 257209 (2003)

22. I.N. Krivorotov, N.C. Emley, A.G.F. Garcia, J.C. Sankey, S.I. Kiselev, D.C. Ralph, R.A. Buhrman, Phys. Rev. Lett. **93**, 166603 (2004)
23. W.F. Brown, Phys. Rev. **130**, 1677 (1963)
24. A. Aharoni, Phys. Rev. **177**, 793 (1969)
25. J.L. Garcia-Palacios, F.J. Lazaro, Phys. Rev. B **58**, 14937 (1998)
26. Z. Li, S. Zhang, Phys. Rev. B **69**, 134416 (2004)
27. D.M. Apalkov, P.B. Visscher, J. Magn. Magn. Mater. **286**, 370 (2005)
28. D.M. Apalkov, P.B. Visscher, Phys. Rev. B **72**, 180405(R) (2005)
29. H.A. Kramers, Physica **7**, 284 (1940)
30. C. Serpico, G. Bertotti, I.D. Mayergoyz, M. d'Aquino, R. Bonin, J. Appl. Phys. **99**, 08G505 (2006)
31. Z. Li, J. He, S. Zhang, Phys. Rev. B **72**, 212411 (2005)
32. L. Perko, *Differential Equations and Dynamical Systems* (Springer-Verlag, New York, 1996)
33. G. Bertotti, C. Serpico, I.D. Mayergoyz, R. Bonin, A. Magni, M. d'Aquino, IEEE Trans. Magn. **41**, 2574 (2005)
34. R. Bonin, G. Bertotti, I.D. Mayergoyz, C. Serpico, J. Appl. Phys. **99**, 08G508 (2006)
35. G. Bertotti, I.D. Mayergoyz, C. Serpico, J. Appl. Phys. **95**, 6598 (2004)
36. G. Bertotti, I.D. Mayergoyz, C. Serpico, Physica B **343**, 325 (2004)
37. C.W. Gardiner, *Handbook of Stochastic Methods* (Springer-Verlag, Berlin, Germany, 1985)
38. R. Kubo, N. Hashitsume, Suppl. Progr. Theor. Phys. **46** (1970)
39. G. Bertotti, I.D. Mayergoyz, C. Serpico, J. Appl. Phys. **99**, 08F301 (2006)
40. R.L. Stratonovich, *Topics in the Theory of Random Noise,* (Gordon and Breach, New York, 1963), Vol. I
41. M.I Freidlin, A.D. Wentzell, Mem. Am. Math. Soc. **109**, No. 523 (2006)
42. S. Mangin, D. Ravelosona, J.A. Katine, M.J. Carey, B.D. Terris, E.E. Fullerton, Nature Mater. **5**, 210 (2006)